Journal of Ultrafine Grained and Nanostructured Materials
https://jufgnsm.ut.ac.ir
Vol. 57, No.1, June 2024, pp. 104-111
Print ISSN: 2423-6845 Online ISSN: 2423-6837
DOI: 10.22059/jufgnsm.2024.01.12

An investigation on microstructures and residual stresses of pure copper sheets fabricated by constrained studded pressing

M. M. Kaykha[1,], SaraSadat Hosseini Faregh[2]*

[1]Department of Mechanical Engineering, Faculty of Engineering, University of Zabol;
[2]Department of Metallurgy and Materials Science, School of Engineering, Shahid Bahonar University of Kerman.

Recieved: 21 March 2024; Accepted: 10 June 2024

**Corresponding author email: mm.kaykha@uoz.ac.ir*

ABSTRACT

One of the newest methods of severe plastic deformation (SPD) is Constrained studded pressing (CSP) method. A limitation of the constrained studded pressing process is the creation of surface cracks on the sheet. One of the most important factors affecting surface cracks is residual stress. In the present study, the effect of residual stresses on delaying the formation of microcracks on the surface and increasing the amount of applied strain on pure copper samples produced by CSP with the use of lubricant was investigated. Therefore, the strain distribution on the copper sheet for the first pass was studied using the finite element method (FEM). In addition, the evaluation of mechanical properties, microstructure, and residual stresses of the samples were studied before and after applying the CSP method. An optical microscope was used to examine the microstructure of the annealed and deformed copper sheets. The average grain size decreased from 35 µm for the annealed sample to 14 µm and 580 nm for the first and tenth passes, respectively. Changes in residual stresses also studied by X-ray diffraction. The residual stresses reached from +197.5 MPa for the annealed sample to -893.9 MPa in the 10th pass sample To check the mechanical properties, the microhardness Vickers test was used. The hardness of the annealed copper sample was 60.87 Vickers, which reached 85.85 VHN and 115 VHN after the first pass and tenth pass, respectively. Moreover, the hardness inhomogeneity factor (H.I.F) was used to calculate the uniformity of the Vickers microhardness distribution. Initially, the H.I.F increased and then decreased for the first pass, which means that the homogeneous distribution of microhardness increased.

Keywords: *Constrained Stud Pressing, Pure Copper Sheet, Residual stress, Grain size, Micro-Crack.*

1. Introduction

Current progress in severe plastic deformation (SPD) methods is directed towards generating metal sheets with ultrafine grain and nanostructures [1-3]. A fundamental aspect of SPD techniques is the consistent preservation of the deformed sample's dimensions during the process. [4]. The most common methods for sheets are accumulative rolling bonding (ARB) [5], Repetitive corrugation and straightening (RCS) [6], and Constrained groove pressing(CGP) [7]. in 2002, CGP was initially planned by Shin et al. [8]. The effective factors of the CGP technique are friction between the groove and sheet, sheet thickness, and geometric shape of the dies. The die design is an operational feature that influences the microstructure and stress distribution. A new method similar to the CGP technique was presented in 2018, which has a higher pressing speed than CGP. This new method is called Constrained Studded Pressing (CSP) [9].

In the CSP method, because of the die geometry, there is no need to rotate the sheet after each pass. Therefore, each pass consists of only two pressing steps. Existing research has shown that different dies with different geometric shapes can be used in the groove pressing method. Because of their different geometry, each of these dies causes different strains in the sheet under intense plastic deformation. Guan and Wang [10] experimentally and numerically investigated the parameters of CGP using the Taguchi optimization method and DEFORM-3D on pure Ni sheets. According to the patterns of peak broadenings, grain refinement occurs, which is consistent with the results of Transmission Electron Microscopy (TEM) observations. Asgari et al. [11] showed that The technique of CGP has demonstrated remarkable efficacy in generating ultrafine grained pure copper sheets, as evidenced by the substantial agreement between experimental and simulation outputs. Tavajjohi and Honarpisheh [12] illustrate that the residual stress on the surface is compressive, whereas on the central layers, the residual stresses are converted into tensile residual stress. Nazari et al. [13] showed that by increasing the number of CGP passes, the density of dislocations increases, whereas grain size and residual stresses decrease. Moradpour et al. [14] performed finite element method (FEM) and experimental validation of CGP and new cross routs on Al-Mg alloy. On the basis of the finite element simulation results, compared to the analytical method, due to the assumption of pure shear conditions and friction values, more strain values were predicted. Furthermore, the experimental results showed that the new method leads to a more uniform and significant change on microstructure of Al-Mg alloy compared with the conventional method. There are many studies on CGP finite element analysis, microstructural evaluation, and mechanical behavior. Nonetheless, the CSP process FEM has not yet been presented. Understanding the residual stress distribution and microstructural evolution in pure copper sheet during CSP is crucial for optimizing the forming process and adjusting material properties for specific applications. Overall, residual stress analysis and microstructure evaluation of pure copper sheet during CSP is a multifaceted research area with implications for enhancing the mechanical properties of materials. By comprehensively understanding the interplay between residual stress distribution, microstructural evolution, and mechanical behavior, researchers can advance the development of high-performance pure copper sheets using an optimized CSP process. In this study, the relationship between residual stress, microstructural evaluation and mechanical behavior of pure copper sheets produced by CSP was investigated using FEM and experiments.

2. Experimental procedure

2.1. CSP process

A schematic of the CSP dies is shown in Figure 1. In the first step, the sheet is pressed with a pair of symmetrical studded dies. In the non-sloping region between the two studs, no deformation is applied, whereas the inclined section of the die is subjected to plane strain and pure shear. In CSP dies, the stud angle is 45°. According to the Von Mises criterion, the applied shear strain in the deformation zone is equal to 0.82 [15]. In the next step,

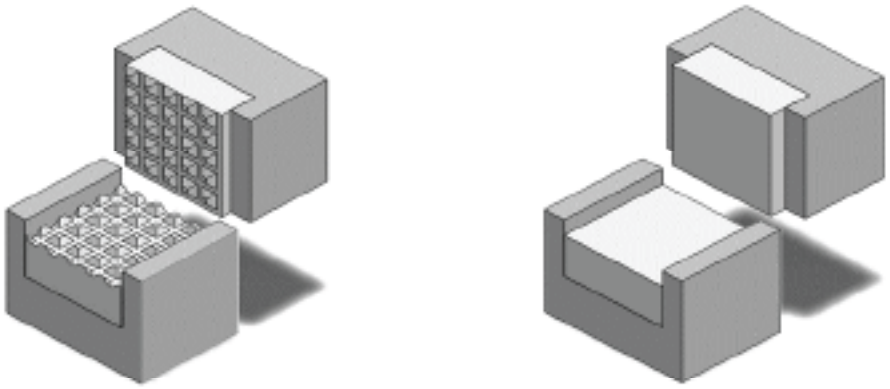

Fig. 1- CSP die set design: (a) studded dies set, (b) flat dies set.

pressing is performed using a flat die, in which, under constrained conditions, the previously deformed region undergoes plastic deformation in reverse. If the area was not deformed in the previous step, it remains unchanged. Pressing with studded and flat dies creates a homogeneous strain. In the CSP method, there is no requirement to rotate and move the sample, and only two pressing steps are used to change the shape of the sheet. The CSP method is faster than the CGP method and applies more strain in each pass. It should be noted that in this research, calcium-based graphite grease was used to reduce the friction between the sheet and the dies.

Figure 2. shows samples of copper sheets of a) corrugated, b) straightened copper sheet for the first pass, and c) straightened copper sheet for the tenth pass respectively.

2.2. Materials and methods:

In this study, commercial pure copper metal with a purity of 99.9% was used. The samples were cut into dimensions of 5 5 cm. To create a homogeneous metallurgical structure and relieve stress, copper sheets were annealed at 650 °C for 2 h. Copper sheets were pressed using a 60-ton hydraulic press at room temperature at a constant speed of 0.1 mm/s. To reduce the friction of the sheet and metal dies, a calcium-based graphite grease lubricant was used. To perform the hardness test, the MH4 Koopa machine was used to implement Vickers hardness tests with an accuracy of ±3 HV. A load of 1 kg was applied for 10 s at equivalent distances of 1 mm from the edge of the sheet with 10 repetitions of measurements. An Olympus BH2 light microscope was used to observe the microstructural changes in the material. Samples with dimensions of 2 x 2 x 1 mm were cut for metallographic samples. After sanding with 200, 500, 800, 1000, 2000, and 2500 sandpapers, the samples were polished using a polishing machine at 100 rpm. Then the samples were washed with alcohol. For etching, a solution consisting of 4 mL HCL, 2 mL HF, 175 mL distilled water, and 20 mL HNO3 was used. X-ray diffraction (XRD) was used to analyze the microstructural characteristics and residual stresses of the samples. For this purpose, the XRD PW1730 machine was used to measure grain size and analyze residual stresses. The XRD PW1730 uses a copper lamp to produce X-ray with a wavelength of 1.54 Å with an accuracy of 0.05 in 2θ. X-ray diffractometer analysis ranges from 10° to 80°, and the peak width at half height, and angle 2θ were calculated. Errors due to the instrumental effect of Warren's method were also calculated.

3. Results and discussion

3.1. Finite Element Analysis:

As shown in Figures 3a and 3b, the effective plastic strain distribution in the CSP method is more homogeneous (comparison of the corrugation step and straightening step of CSP for the first pass). According to the CSP die geometry, the effective strain values from the simulations are similar to those in the CSP process section. As shown in Figures 3a and 3b, in the CSP method, the maximum effective strain occurred in the inclined region of the stud and was approximately 0.79, and for the straightening step, it was approximately 1.2. According to the effective plastic strain results of the CSP method, the types of deformations for the CGP and SCP methods are completely different from each other; therefore, in the CGP method, the deformation occurs along the grooves, but in the CSP method, it

a b c

Fig. 2- copper sheets produced by CSP dies: a) corrugated copper sheet, b) straightened copper sheet for the first pass and c) straightened copper sheet for the tenth pass.

occurs around the studs [15].

3.2. Microstructure evaluation

Figure (4-a) shows the optical microscopy image of the annealed copper sample. Figures (4-b) and (4-c) show the CSP copper samples for the first and tenth passes, respectively. The average grain size decreased from 35 μm in the annealed sample

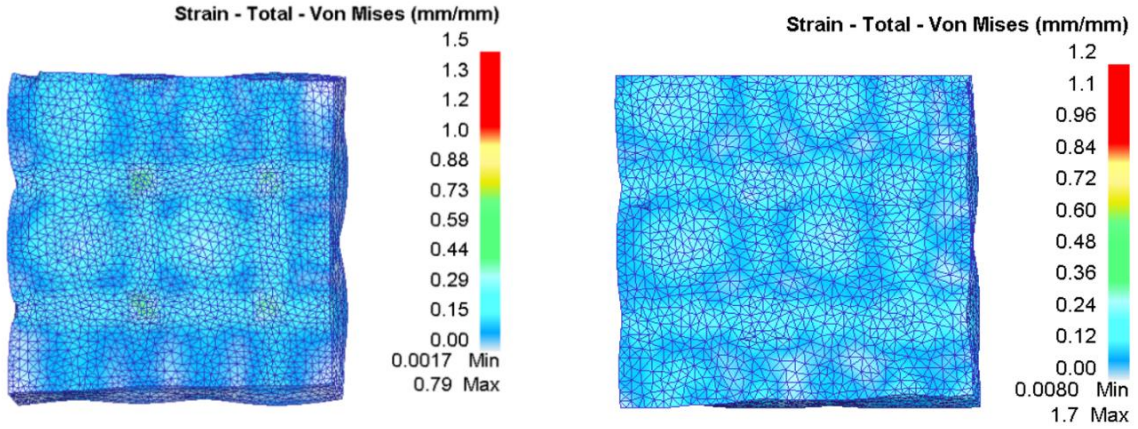

a b

Fig. 3- Effective plastic strains distribution for a) corrugation step and b) straightening of CSP.

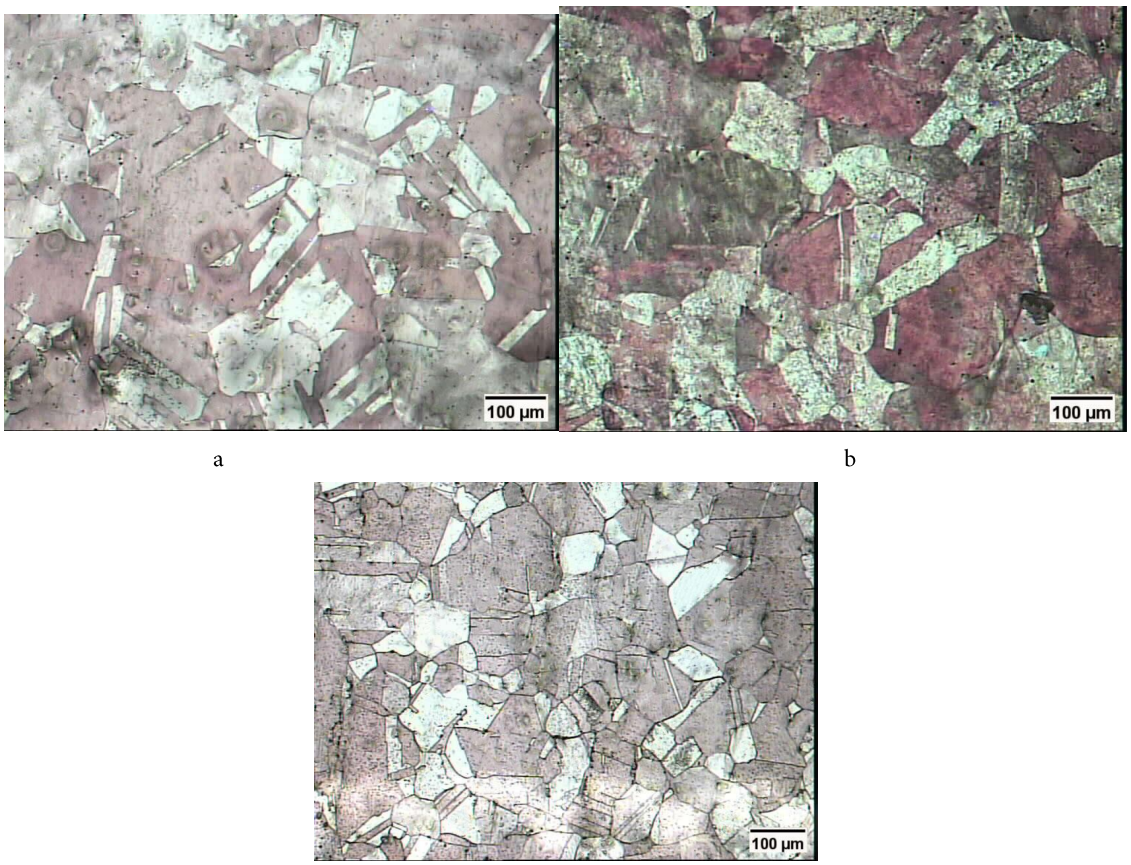

a b

c

Fig.4- Optical micrographs of samples a) as-received, b) first pass and, c) 10 pass of CSP process.

to 14 μm after the first CSP pass. In the 10th pass, due to the sharp decrease in grain size, XRD test results were used with the applying of Williamson Hall method to calculate the grain size. The average crystallite size decreases to 580 nm in the 10th pass. According to Figure (4-c), considering the increase of the applied intense strain in the 10th pass and taking into account the fact that, the mechanism of grain refinement is based on the effect of large plastic deformation on the microstructure evolution. Therefore, the values of the density of dislocations in the 10th pass will experience significant changes [16]. The CSP technique increases the number of existing dislocations compared with the annealed sample under intense strain. As the density of dislocations increases, the driving force increases. Subsequently, the dynamic recovery also increases [17]. Since dynamic recovery is proportional to dislocation density, dynamic recovery removes dislocations. As a result, by applying more strain and increasing the dynamic recovery rate following the increase in the density of dislocations, a microstructure consisting of low-angle boundaries and sub-grains is created. This reduction in the size of the crystals and the formation of subgrains causes dislocations to migrate from inside the cells to inside the cell walls [18-20].

3.3. XRD Analysis

Figure (5) illustrates the XRD curves for the annealed sample and the first and tenth passes of the CSP process. Compared with the annealed sample, in the first pass of the CSP, by applying high strain and increasing the strain amounts in the tenth pass, the width of the peaks increased. One of the most important reasons for the increase in the width of the peaks in the XRD patterns is the severe plastic deformation and grain refinement [21]. Due to the intense severe strain caused by the CSP process, the distance between the crystallographic plane changes [22]. Due to the fact that more strain can be applied to the sample by the CSP technique, the slip levels in FCC structures increase. Therefore, we can refer to the shear nature of severe plastic deformation [23]. The highest XRD intensity was obtained from the diffraction of the crystal planes (1 1 1), (0 0 2), and (0 2 2). One of the interesting points related to the changes in the XRD curves is the change in the distance between the plates. This change caused the transformation of the maximum intensity in the XRD spectrum from (200) to (111).

3.4 Residual stresses

Figure (6) shows the X-ray diffraction intensity diagrams in terms of 2θ angle for three samples of pure annealed copper and CSPed copper by applying one and ten passes. The results show a decrease in the tensile residual stress values from +197.5 MPa in the annealed sample to -703.7 MPa in the first pass sample. By increasing the number of passes, the compressive residual stress was reduced to 893.9 MPa in the last pass. In the tenth pass of plastic deformation, compressive residual stresses are created. The main cause of residual stress is the heterogeneous deformation of the material on macroscopic and microscopic scales. Usually, the presence of tensile residual stresses near the surface of parts exposed to alternating loads reduces the fatigue life of these materials. Conversely, the presence of compressive residual stresses postpones fatigue life by preventing the formation and growth of cracks [24]. Compressive residual stresses can also improve resistance to wear and corrosion [25]. For CSPed sheets, there is a tensile residual stress for

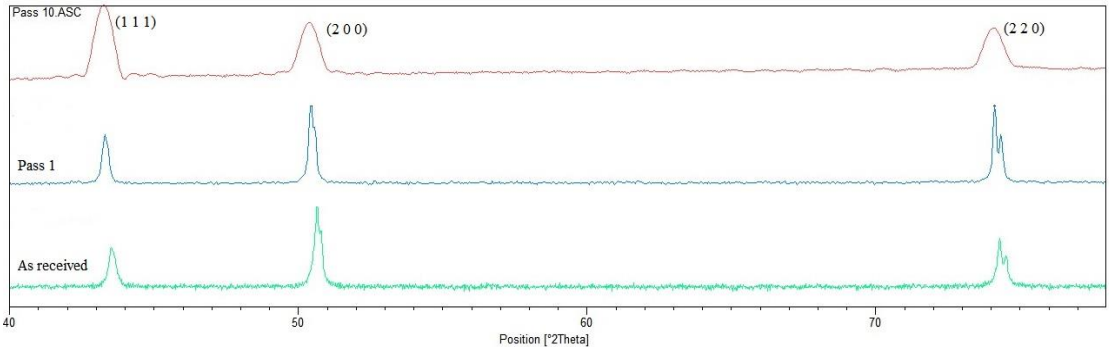

Fig. 5- X-ray diffraction patterns of as received, first, and ten passes.

the initial pass, while by increasing the number of passes, compressive residual stress is created. These compressive residual stresses increase the resistance to crack growth in the production sheets. As the residual stress increases and the type of residual stress changes to compressive, the diffraction patterns becomes wider [25].

3.5. Hardness

Figure 7 displays the Vickers microhardness (VHN) eor the CSPed samples. The hardness of the annealed copper sheet was 60.87 Vickers, which reached 85.85 Vickers after the first pass. The microhardness value in the final pass reached a maximum value of 115 Vickers. the hardness inhomogeneity factor (H.I.F) using the following equation was used to calculate the uniformity of the Vickers microhardness distribution [26]:

$$HIF = (\sqrt{(\sum_{i=1}^{n}(H_i - \overline{H})^2)/(n-1)})/\overline{H} \quad (1)$$

where is the number of hardness measurements on each pass, is the hardness value at measurement, and is the mean hardness value. Figure 8 shows the H.I.F for the CSP samples. As shown, initially the H.I.F increased for the first pass and then decreased (that is, the homogeneous distribution of microhardness increased).

4. Conclusions

In this study, the influence of the CSP process on the mechanical properties, microstructure, and residual stresses was investigated for copper sheets. For this purpose, Vickers microhardness tests, optical microscopy, and X-ray diffraction patterns were used, the results of which are summarized below:

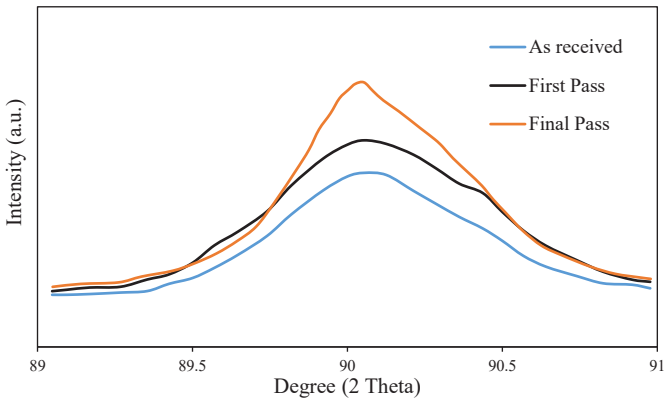

Fig. 6- XRD patterns for residual stress (a) as received, (b) first, and (c) final passes.

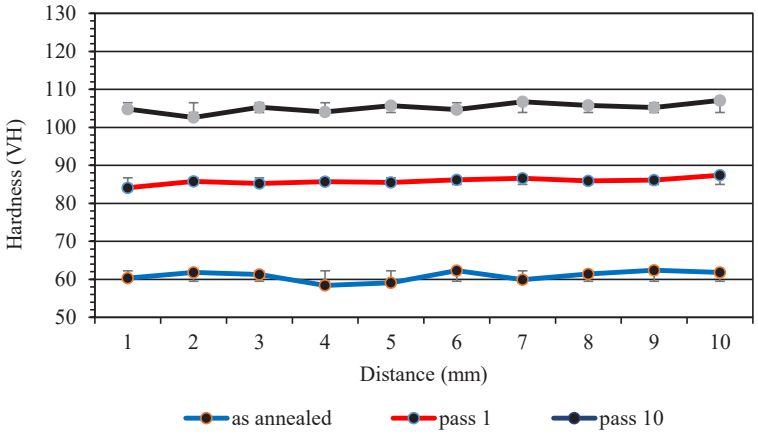

Fig. 7- Distribution of Vickers microhardness along the direction.

1. Finite element simulation of the CSP method showed that with the help of the CSP process, strain values of approximately 1.2 can be applied to the copper sample.

2. The hardness of the annealed copper sample was 60.87 Vickers, which reached 85.85 VHN and 115 VHN after the first pass and tenth pass, respectively. For the final pass, the homogeneous distribution of the microhardness increased.

3. The average grain size decreased from 35 μm in the annealed sample to 14 μm in the first pass sample. Finally, in the tenth pass, the average grain size decreased to 580 nm.

4. By applying high strain values, according to the geometry of the CSP dies;, the accumulation of dislocations increases. Increasing the density of dislocations led to a more dynamic recovery.

5. Residual stresses reached from +197.5 MPa for the annealed sample to 899 MPa in the 10th pass sample.

6. By increasing the number of passes, the residual stress values altered from tensile to compressive which can delay the growth of cracks.

7. Decreasing the grain size causes the broadening of the peaks.

8. With increasing effective plastic strain values, the distance between the crystal planes has also changed. This change shifted the maximum intensity in the XRD spectrum from (200) plane to (111).

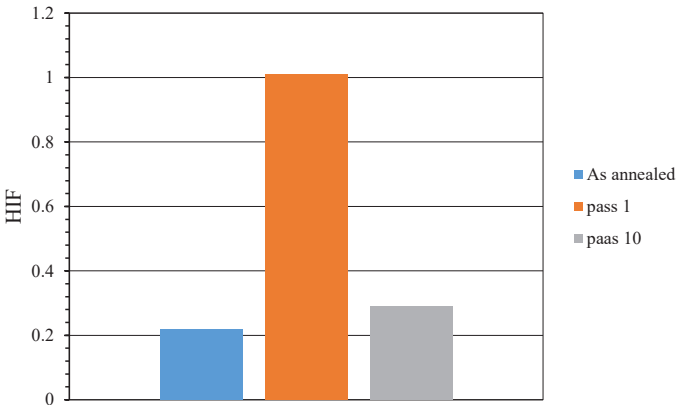

Fig. 8- HIF for the as-annealed sample, first and tenth passes.

References

1. Mollaei, N., et al. *"Zinc based bioalloys processed by severe plastic deformation – A review."* Journal of Ultrafine Grained and Nanostructured Materials ,(2020).53(1): p.39-47.

2. Esbolat, A., et al. "Development of Asymmetric Rolling as a Severe Plastic Deformation Method: A Review." Journal of Ultrafine Grained and Nanostructured Materials. (2022). 55(2): 97-111.

3. Sarkari Khorrami, M.. "Friction stir welding of ultrafine grained aluminum alloys: a review." Journal of Ultrafine Grained and Nanostructured Materials ,(2021), 54(1): 1-20.

4. Ebrahimi GR, Barghamadi A, Ezatpour HR, Amiri A. A novel single pass severe plastic deformation method using combination of planar twist extrusion and conventional extrusion. Journal of Manufacturing Processes. 2019;47:427-36.

5. Saito Y, Tsuji N, Utsunomiya H, Sakai T, Hong RG. Ultra-fine grained bulk aluminum produced by accumulative roll-bonding (ARB) process. Scripta Materialia. 1998;39(9):1221-7.

6. Zhu YT, Jiang H, Huang J, Lowe TC. A new route to bulk nanostructured metals. Metallurgical and Materials Transactions A. 2001;32(6):1559-62.

7. Shin DH, Park J-J, Kim Y-S, Park K-T. Constrained groove pressing and its application to grain refinement of aluminum. Materials Science and Engineering: A. 2002;328(1-2):98-103.

8. Shin DH, Park J-J, Kim Y-S, Park K-T. Constrained groove pressing and its application to grain refinement of aluminum. Materials Science and Engineering: A. 2002;328(1-2):98-103.

9. Torkestani A, Dashtbayazi MR. A new method for severe plastic deformation of the copper sheets. Materials Science and Engineering: A. 2018;737:236-44.

10. Guan Y, Wang Z. Numerical and Experimental Study on Constrained Groove Pressing. Severe Plastic Deformation Techniques: InTech; 2017.

11. Asgari, M., M. Honarpisheh, and H. Mansouri, *Experimental and Numerical Investigation of Mechanical Properties in the Ultrasonic Assisted constraint groove pressing process of copper sheets.* Journal of Ultrafine Grained and Nanostructured Materials, 2020. 53(1): p. 48-59.

12. Tavajjohi MH, Honarpisheh M. Experimental and numerical study of the longitudinal and transverse residual stresses distribution in the constrained groove pressing process of pure copper sheets. Proceedings of the Institution of Mechanical En-

gineers, Part L: Journal of Materials: Design and Applications. 2021;236(1):97-109.
13. Nazari F, Honarpisheh M, Zhao H. The effect of microstructure parameters on the residual stresses in the ultrafine-grained sheets. Micron. 2020;132:102843.
14. Moradpour M, Khodabakhshi F, Mohebpour SR, Eskandari H, Haghshenas M. Finite element modeling and experimental validation of CGP classical and new cross routes for severe plastic deformation of an Al-Mg alloy. Journal of Manufacturing Processes. 2019;37:348-61.
15. Torkestani A, Dashtbayazi MR. A new method for severe plastic deformation of the copper sheets. Materials Science and Engineering: A. 2018;737:236-44.
16. Mirzadeh, H. "Superplasticity of fine-grained austenitic stainless steels: A review." Journal of Ultrafine Grained and Nanostructured Materials, (2023).56(1): p.27-41.
17. Humphreys, F.J. and M. Hatherly, *Recrystallization and related annealing phenomena*. 2012: elsevier.
18. Krishnaiah A, Chakkingal U, Venugopal P. Production of ultrafine grain sizes in aluminium sheets by severe plastic deformation using the technique of groove pressing. Scripta Materialia. 2005;52(12):1229-33.
19. Satheesh Kumar SS, Raghu T. Strain path effects on microstructural evolution and mechanical behaviour of constrained groove pressed aluminium sheets. Materials & Design. 2015;88:799-809.
20. Hosseini Faregh SS, Raiszadeh R, Dashtbayazi MR. Pure Copper Sheets Processed by Constrained Studded Pressing: The Effect of Die Angle. Journal of Materials Engineering and Performance. 2023;33(7):3262-72.
21. Cullity BD, Smoluchowski R. *Elements of X-Ray Diffraction*. Physics Today. 1957;10(3):50-.
22. Mou X, Peng K, Zeng J, Shaw LL, Qian KW. The influence of the equivalent strain on the microstructure and hardness of H62 brass subjected to multi-cycle constrained groove pressing. Journal of Materials Processing Technology. 2011;211(4):590-6.
23. Pouraliakbar H, Jandaghi MR, Mohammadi Baygi SJ, Khalaj G. Microanalysis of crystallographic characteristics and structural transformations in SPDed Al Mn Si alloy by dual-straining. Journal of Alloys and Compounds. 2017;696:1189-98.
24. Totten, G.E., *Handbook of residual stress and deformation of steel*. 2002: ASM international.
25. Rossini NS, Dassisti M, Benyounis KY, Olabi AG. Methods of measuring residual stresses in components. Materials & Design. 2012;35:572-88.
26. Kaykha MM, Dashtbayazi MR. An Improvement in Constrained Studded Pressing for Producing Ultra-Fine-Grained Copper Sheet. Metals. 2022;12(2):193.